DALTON
FULL PAPER

# Pinch-porphyrins, new spectroscopic and kinetic models of peroxidases

**Yasmi Reyes-Ortega,*[a,b] Cecilio Alvarez-Toledano,[b] Daniel Ramírez-Rosales,[c] Amparo Sánchez-Sandoval,[a] Enrique González-Vergara[a] and Rafael Zamorano-Ulloa[c]**

[a] *Centro de Química del Instituto de Ciencias, Benemérita Universidad Autónoma de Puebla, México*
[b] *Instituto de Química, Universidad Nacional Autónoma de México, México*
[c] *Escuela Superior de Física y Matemáticas, Instituto Politécnico Nacional, México*

The novel complexes [1,9-bis(2-pyridyl)-2,5,8-triazanonane]-(protoporphyrinato)iron(III) **4**, -(mesoporphyrinato)-iron(III) **5** and -(deuteroporphyrinato)iron(III) **6** were synthesized from the parent compounds chloro-(porphyrinato)iron(III) **1**, -(mesoporphyrinato)iron(III) **2** and -(deuteroporphyrinato)iron(III) **3** and 1,9-bis(2-pyridyl)-2,5,8-triazanonane (picdien). The complexes **1**–**6** were characterized by UV/VIS, $^1$H NMR and ESR spectroscopies and their catalytic activity was determined. The measured theoretical maximum rate constant ($k_{cat}$) for guaiacol + $H_2O_2$ ⟶ oxidation guaiacol products (guaiacol = 2-methoxyphenol) in the presence of complexes **4**–**6**, were $7.6 \times 10^6$, $4.4 \times 10^5$ and $9.0 \times 10^4$ mol$^{-1}$ s$^{-1}$, respectively. These peroxidase activities are to our knowledge the largest reported for model complexes. The UV/VIS spectra show Soret and Q bands for all compounds at energies typical of axially co-ordinated complexes with symmetry $D_{4h}$ or lower. The intensity of the charge-transfer transitions indicates that the presence of the picdien ligand diminishes the distortion of the parent compounds. The $^1$H NMR spectra of complexes **4**–**6** are indicative of six-co-ordinated complexes with different degrees of quantum mixed-spin (qms) state $S = \frac{5}{2}$ into $S = \frac{3}{2}$. The ESR spectral features are characteristic of qms species, A and B, for each compound. Maltempo's theory for qms states gives the admixture percentage of species A (53–64%) and species B (<8%) for each compound. The area ratio of the ESR B : A signals follows the same order as the peroxidase activity shown by these complexes. A clear correlation is established among the peroxidase activity, the iron(III) out-of-porphyrin plane configuration and the qms state $S = \frac{5}{2}$ and $S = \frac{3}{2}$.

The different co-ordination structures of the iron–heme proteins show many magnetic states of the iron that in turn correlate with the biochemical behavior of the compound.[1–4] This variety of compounds and behaviors has been a generous source of knowledge.[5–24] The existence of three possible spin states for the five d electrons of iron(III) in these compounds has been established, namely: the pure high-spin state $S = \frac{5}{2}$,[8,10,14,15,19,21] the pure low-spin state $S = \frac{1}{2}$[9,12,13,15,19–21] and the quantum mixed-spin state $|\text{qms}\rangle = \alpha|\frac{5}{2}\rangle + \alpha'|\frac{3}{2}\rangle$.[4–7]

Pure high spin $S = \frac{5}{2}$ $Fe^{III}$ five-co-ordinated porphyrins are obtained when one weak-field ligand is axially co-ordinated to the iron–heme group. This weak-field ligand produces the contraction of the porphyrin ring and the displacement ($r_{Fe} \approx 0.5$ Å) of the iron ion out of the heme plane[25] and the measured peroxidase activity is low (<$10^5$ mol$^{-1}$ s$^{-1}$).[11] Frequently, these compounds undergo rapid irreversible autooxidation reactions precluding the oxidation of other substrates.[25]

For Fe–heme compounds that axially co-ordinate two weak-field ligands, the porphyrin ring expands and the iron ion gets closer to the heme-plane, $r_{Fe} \longrightarrow 0$, and the molecular symmetry tends toward $O_h$. Thus, the electronic properties of these six-co-ordinated complexes might differ from those of the five-co-ordinated anion-bound derivatives.[25]

The first biological enzyme recognized as a qms state system was chromatium ferricytochrome c′ peroxidase, reported by Maltempo *et al.*[4,26] After this pioneering work, other Fe–heme qms systems have been reported, some examples are: peroxidase enzymes,[5–7] five- and six-co-ordinate complexes,[25,27–35] and dimer derivatives.[36] In addition, compounds showing a thermal mixture of the pure states $S = \frac{5}{2}$ and $\frac{1}{2}$ have also been reported.[4] These systems can be readily recognized by their thermal behavior.

In 1977[34] reports appeared on $Fe^{III}$ porphyrins five-co-ordinated to weak-field anions that have been characterized as qms systems which show magnetic properties that span a continuum of magnetic states between the pure $\frac{1}{2}$ and the pure $\frac{5}{2}$ spin states. Recently, Reed and Guiset[1] have proposed a qualitative magnetochemical series based on the iron ligand field deduced from the mixing of $S = \frac{3}{2}$, $\frac{5}{2}$ spin states in porphyrin–iron(III) compounds.

## Results and Discussion

Based on the above, we consider it of great importance to synthesize models of six-co-ordinated iron–porphyrin complexes possessing quantum mixed spin states $|\frac{5}{2}\rangle$ and $|\frac{3}{2}\rangle$ which could show substantial catalytic peroxidase activity. It is considered that such spin states can be obtained by the selective co-ordination of weak-field chain ligands, where the length of the chain controls the co-ordination strength towards $Fe^{III}$. This in turn will affect the distortion and the heme plane displacement of the metallic ion.

For such reasons, three novel complexes were obtained from the parent compounds chloro-(protoporphyrinato)iron(III) **1**, -(mesoporphyrinato)iron(III) **2** and -(deuteroporphyrinato)-iron(III) **3** axially co-ordinated with 1,9-bis(2-pyridyl)-2,5,8-triazanonane (picdien) [Fig. 1(*a*) and 1(*b*)], which will be named pinch-porphyrins from now on (Fig. 2).

### UV/VIS spectroscopy

The UV/VIS spectra of complexes **1** and **4** are shown in Fig. 3. An intense Soret band and two weak Q bands indicate that the complexes have $D_{4h}$ or lower symmetry.[37–40] The spectra of the other complexes (**2**, **3**, **5** and **6**) are similar to those in Fig. 3. For compounds **4**–**6** the Soret line is at 399.4, 388.0 and 387.4 nm

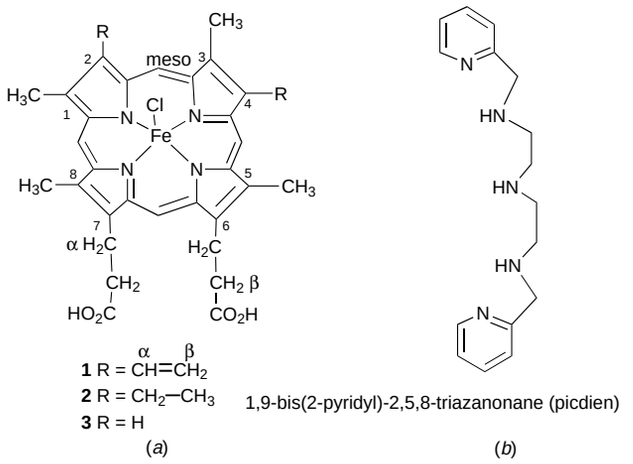


**Fig. 1** (*a*) Chloro(protoporphyrinato)iron(III) **1**; chloro(mesoporphyrinato)iron(III) **2**; chloro(deuteroporphyrinato)iron(III) **3**. (*b*) 1,9-Bis(2-pyridyl)-2,5,8-triazanonane (picdien)

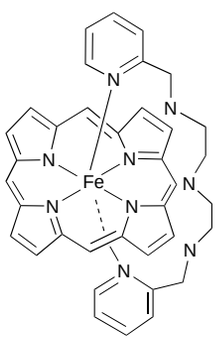


**Fig. 2** Proposed structure for pinch-porphyrins. The substituent groups are not indicated in the figure for clarity

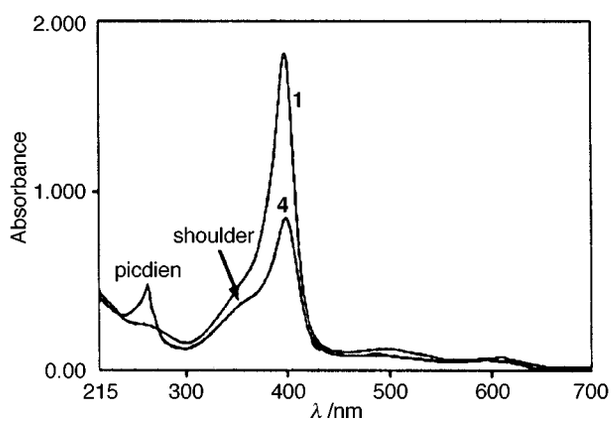


**Fig. 3** The UV/VIS spectra of complexes **1** and **4**

respectively and the Q bands are at 486 and 593.8 (**4**), 480 and 584 (**5**) and 479.8 and 590 nm (**6**). The compounds **4**–**6** show one shoulder at 358, 342.5 and 344.5 nm respectively with intensities (*I*) $I_4 \ll I_5 < I_6$, these shoulders are not present in the UV/VIS spectra of the parent compounds **1**–**3** (Table 1); however, they do appear in the UV/VIS spectra of the native enzymes.[40,41]

For the picdien-free porphyrin–iron complexes **1**–**3**, the spectra are characteristic of porphyrin–iron(III) systems.[37–40] The UV/VIS spectra of compounds **4**–**6** are less intense than the spectra of compounds **1**–**3** indicating, in accord with Solomon *et al.*,[42] that the amount of distortion of the ligand field into the ligand field excited state, is diminished.

### Proton NMR spectroscopy

Table 2 summarizes the $^1$H NMR data of spectra taken at room temperature in $CD_3OD$ solvent. The assignment of the signals

**Table 1** Optical absorption spectra of complexes of porphyrin–iron(III) and porphyrin–iron(III)–picdien

| | $\lambda_{max}$(MeOH)/nm | | | |
|---|---|---|---|---|
| Iron–porphyrin | Shoulder | Soret | Band $Q_1$ | Band $Q_2$ |
| **1** | | 397.4 | 498.0 | 615.0 |
| **4** | 358.0 | 399.4 | 486.0 | 593.8 |
| **2** | | 377.2 | 485.6 | 593.0 |
| **5** | 342.5 | 388.0 | 480.0 | 584.0 |
| **3** | | 386.5 | 488.0 | 589.0 |
| **6** | 344.5 | 387.4 | 479.8 | 590.0 |

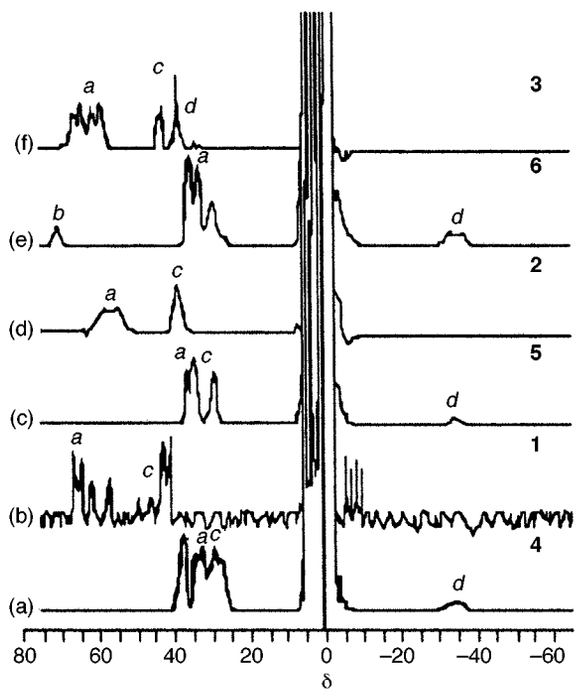


**Fig. 4** The 500 MHz $^1$H NMR spectra of complexes (a) **4**, (b) **1**, (c) **5**, (d) **2**, (e) **6** and (f) **3**. In all cases, the heme substituents are labeled *a*, heme-$CH_3$; *b*, 2,4-H; *c*, α-$CH_2$; *d*, meso-H [14,15,43–45]

for the six compounds (**1**–**6**) were based on analogous model compounds previously reported.[14,15]

The spectra of the three chloro(porphyrinato)iron(III) complexes **1**–**3**, recorded at concentrations of *ca.* $10^{-2}$ mol dm$^{-3}$ in $CDOD_3$ at 27 °C, show the averaged signals of the porphyrin–$Fe^{III}$ co-ordinated to chloride and/or to $CD_3OD$, and aggregates of the type porphyrin–Cl–porphyrin.[15]

For compounds **4**–**6**, in accord with Hill and Morallee,[9] the results show that at low temperature the species in solution are bis(pyridinato)iron(III) porphyrins. At higher temperature (*ca.* 290 K), fast equilibrium between the different species is present and the averaged signals are observed for free and co-ordinated pyridines.[9]

The chemical shift values of the four heme-methyl groups are often assigned on the basis of intensity and high frequency positions. These are thus quite sensitive to the $S = \frac{3}{2}$ and $S = \frac{5}{2}$ contributions in a spin-admixed compound because unpaired spin in the $d_{x^2-y^2}$ orbital is associated with predominant σ-spin delocalization and high frequency pyrrole proton isotropic shifts.[28]

The methyl-heme and the meso-proton resonances of the picdien-free porphyrin–iron compounds **1**–**3** have chemical shifts associated with a high-spin $Fe^{III}$ complex [Fig. 4(b), 4(d), 4(f) and Table 2].[1,15,43–45] This is a consequence of the added effect of the π-electron mechanism on a dominant σ-electron mechanism.[43–47]

The chemical shifts assigned to the methyl-heme and the meso-protons of the picdien–porphyrin–iron complexes **4**–**6**

**Table 2** Proton NMR data* of iron–porphyrins and their picdien complexes

| Compound | $\delta_{heme\text{-}CH_3}$ *a* | Spread $\delta_{heme\text{-}CH_3}$ | Average $\delta_{heme\text{-}CH_3}$ | $Q_{asym}$ | $\delta_{2,4\text{-}H}$ *b* | $\delta_{meso\text{-}H}$ *d* | $\delta_{\alpha\text{-}CH_2}$ *c* |
|---|---|---|---|---|---|---|---|
| **1** | 71.39 | | | | | | |
| | 70.46 | | | | | | |
| | 66.93 | | | | | | |
| | 62.03 | 9.00 | 67.70 | 0.13 | | 47–47.6 | 51.61 |
| **4** | 42.21 | | | | | | |
| | 42.21 | | | | | | |
| | 38.71 | | | | | | |
| | 37.93 | 4.28 | 40.26 | 0.10 | | −32.05 | 35.67 |
| **2** | 62.98 | | | | | | |
| | 62.98 | | | | | | |
| | 61.17 | | | | | | |
| | 60.39 | 2.60 | 61.89 | 0.04 | | | 43.47 |
| **5** | 40.34 | | | | | | |
| | 40.34 | | | | | | |
| | 39.13 | | | | | | |
| | 39.13 | 1.21 | 39.73 | 0.03 | | −33.35 | 33.59 |
| **3** | 74.60 | | | | | | |
| | 71.02 | | | | | | |
| | 66.57 | | | | | | |
| | 61.97 | 12.63 | 70.04 | 0.18 | | 37–38.79 | 45–48.5 |
| **6** | 39.62 | | | | | | |
| | 39.62 | | | | | | |
| | 38.25 | | | | | | |
| | 33.59 | 6.03 | 37.77 | 0.16 | 76.40 | −32.44 | 33.59 |

* Spectra were registered on free iron–porphyrin methanolic solutions and after addition of picdien ligand at 25 °C; $\delta_H$(500 MHz; $CD_3OD$; $SiMe_4$).

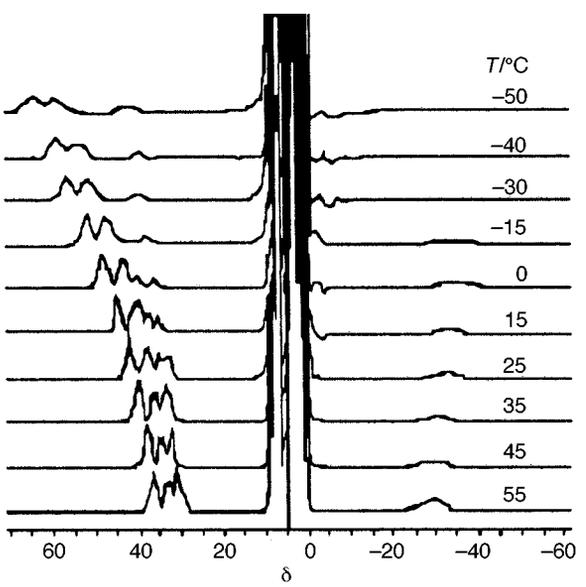


**Fig. 5** The 500 MHz $^1H$ NMR spectra of complex **4** in $CD_3OD$ (referenced to $SiMe_4$) at variable temperatures

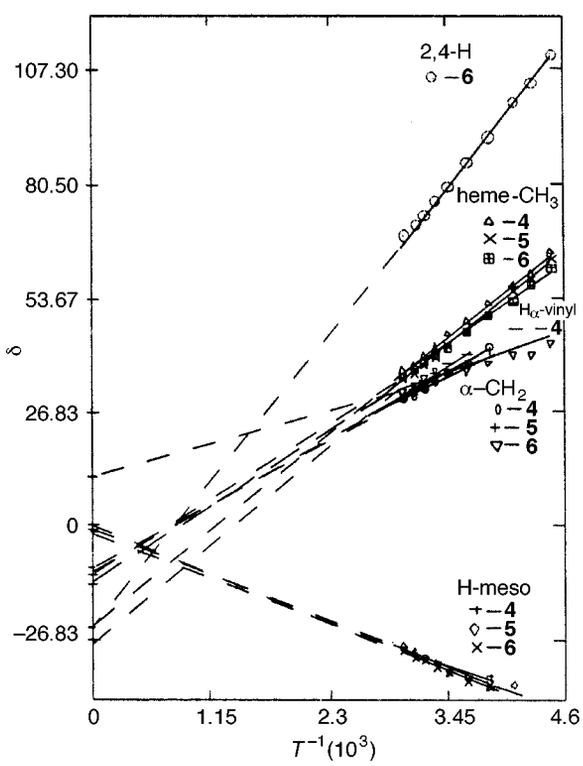


**Fig. 6** Curie law plots of $\delta_{heme\text{-}CH_3}$, $\delta_{H\text{-}meso}$, $\delta_{heme\text{-}vinyl}$, $\delta_{2,4\text{-}H}$ and $\delta_{\alpha\text{-}CH_2}$ of complexes **4**–**6** *vs.* $T^{-1}$, chemical shifts referenced to $SiMe_4$

have been previously interpreted as being due to spin admixed systems.[2,28] These values would indicate that the picdien pyridyl groups have established a weak ligand field that induces some intermediate spin $S = \frac{3}{2}$ character [Fig. 4(a), 4(c) and 4(e)].[2,28,31–35]

Variable-temperature measurements support, clearly, the qms for compounds **4**–**6**. Fig. 5 shows the variation of the chemical shifts of complex **4** with temperature. Fig. 6 shows the linear behavior of the isotropic shifts *vs.* $T^{-1}$ of the different groups of compounds **4**–**6**. The $CH_3$, vinyl-$H_\alpha$, α-$CH_2$ and 2,4-H substituents on pyrrole yield straight lines with essentially non-zero intercepts indicating deviation from Curie behavior as shown by six-co-ordinate porphyrin–iron complexes similar to compounds **4**–**6** but where the Cl has been replaced by two dmso ligands that lie in axial positions.[14] The vinyl-Hα chemical shifts for compound **4** show large deviations (−15.88 ppm for $T^{-1} = 0$) from Curie behavior and are within the expected values, *i.e.* lower than the high-spin, $\frac{5}{2}$, porphyrin–$Fe^{III}$ system.[14]

For the three complexes **4**–**6** the negative meso-H chemical shifts indicate that the picdien ligand has induced a strong $S = \frac{3}{2}$ character. As the temperature is lowered, several tendencies are observed. The heme-$CH_3$ shifts for compounds **4**–**6** increase linearly with a positive slope, but this is smaller than the slope of the pyrrole proton (2,4-H Curie curve) of compound **6**.

The heme-$CH_3$ chemical shift spread produced by the three neighboring peripheral functional groups increases in the order

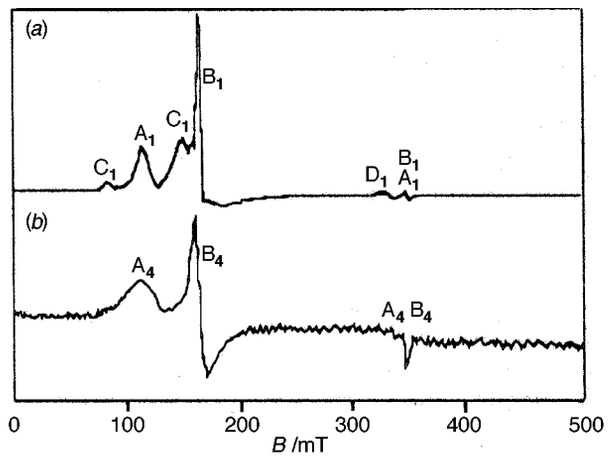


**Fig. 7** The ESR spectra of (*a*) complex **1** with the signals $A_1$, $B_1$, $C_1$ and $D_1$, and (*b*) complex **4** with the signals $A_4$ and $B_4$

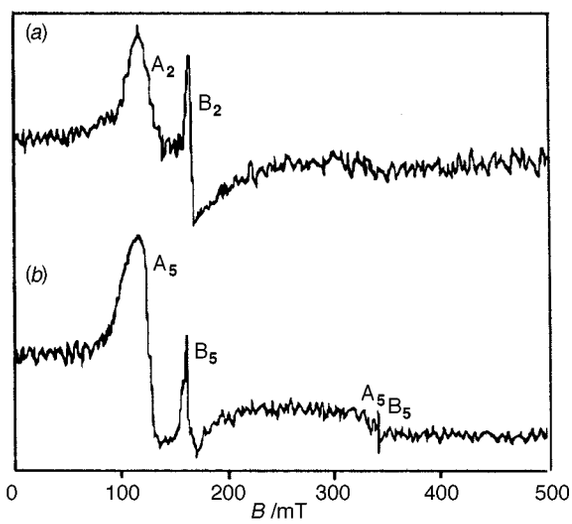


**Fig. 8** The ESR spectra of (*a*) complex **2** with the signals $A_2$, $B_2$, $C_2$ and $D_2$, and (*b*) complex **5** with the signals $A_5$ and $B_5$

ethyl < proton ≈ vinyl as R becomes more electron withdrawing (Fig. 1).[14]

The asymmetry factor [$Q_{asym}$ = (spread heme-$CH_3$)/(average $\delta_{heme\text{-}CH_3}$)][14] is small for compounds **1**–**6** and agrees with the literature values.[14] This indicates that the asymmetry parameter has a value typical of six-co-ordinated complexes.[14]

## ESR spectroscopy

The ESR spectra at X-band of compounds **1**–**6** are shown in Figs. 7–9. The ESR spectrum of **1** in Fig. 7(*a*) shows several signals that have been assigned to at least four different species: three axial species $A_1$ with $g_{\|}^{A_1} = 1.924$ and $g_{\perp}^{A_1} = 5.403$; $B_1$, $g_{\|}^{B_1} = 1.924$ and $g_{\perp}^{B_1} = 4.000$; $C_1$ with $g_{\|}^{C_1} = 7.955$ and $g_{\perp}^{C_1} = 4.000 \pm 0.008$; and a low-spin species $D_1$; $S = \frac{1}{2}$, with $g \approx 2$. After addition of 0.2 mmol picdien to 0.2 mmol protoporphyrin to yield compound **4**, the spectrum of Fig. 7(*b*) was obtained. It shows two new axial species $A_4$ and $B_4$ with $g_{\|}^{A_4} = 1.990$, $g_{\perp}^{A_4} = 5.172$ and $g_{\|}^{B_4} = 1.951$, $g_{\perp}^{B_4} = 4.072$. The low-spin species $C_1$ and $D_1$ present in the parent protoporphyrin compound have disappeared completely in this complex. The large change in the protoporphyrin ESR spectrum caused by the addition of picdien implies a substantial alteration of the ligand environment caused by picdien binding at or near the iron site.

The ESR spectrum of mesoporphyrin–$Fe^{III}$ **2** in Fig. 8(*a*) shows two signals $A_2$ and $B_2$ with $g_{\perp}^{A_2} = 4.890$ and $g_{\perp}^{B_2} = 3.992$. After addition of 0.2 mmol picdien to 0.2 mmol mesoporphyrin–$Fe^{III}$ to yield compound **5**, the spectrum of Fig. 8(*b*) was observed with two axial species $A_5$ and $B_5$ with $g_{\|}^{A_5} = 1.987$, $g_{\perp}^{A_5} = 5.222$ and $g_{\|}^{B_5} = 1.953$, $g_{\perp}^{B_5} = 4.067$.

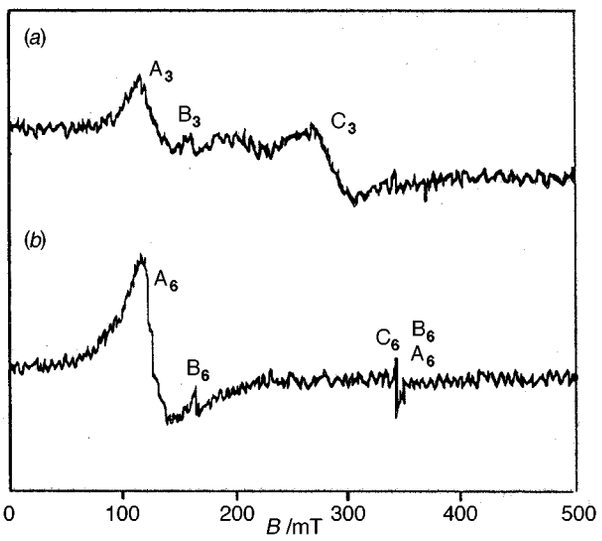


**Fig. 9** The ESR spectra of (*a*) complex **3** with the signals $A_3$, $B_3$ and $C_3$, and (*b*) complex **6** with the signals $A_6$, $B_6$ and $C_6$

Fig. 9(*a*) shows the ESR spectrum of deuteroporphyrin–$Fe^{III}$ **3** with three main signals $A_3$, $B_3$, $C_3$ at $g^{A_3} = 5.137$, $g^{B_3} = 4.117$ and $g^{C_3} = 2.316$. Signal $C_3$ is assigned to a low-spin, $S = \frac{1}{2}$ $Fe^{III}$ species. Once again, substantial changes in the spectrum are observed after addition of 0.2 mmol picdien to 0.2 mmol deuteroporphyrin–$Fe^{III}$ to yield compound **6** as shown in Fig. 9(*b*). Signals $A_6$, $B_6$ and $C_6$ have $g_{\|}^{A_6} = 1.957$, $g_{\perp}^{A_6} = 5.238$, $g_{\|}^{B_6} = 1.957$, $g_{\perp}^{B_6} = 4.100$ and $g^{C_6} = 2.000$. The signal $C_6$ is assigned to a free radical species.

The several ESR species shown by compound **1**, probably correspond to five-co-ordinated chloride or five-co-ordinated methanol complexes, a six-co-ordinated chloride and methanol complex and a six-co-ordinated bis(methanol) complex.[14,48] Several differences and similarities emerge after inspection of these ESR spectra. (*a*) More precisely, the compounds **1**–**3** stabilize similar ESR species labeled $S_1^{A'}$, $S_1^{B'}$, $S_2^{A'}$, $S_2^{B'}$, $S_3^{A'}$, $S_3^{B'}$ and so on, with spectroscopic values summarized in Table 3. (*b*) In all three cases, the addition of the picdien ligand changes the ESR response substantially, giving rise to simpler spectra formed by a pair of axial species A and B for each compound **4**–**6**. (*c*) Signals A and B of the picdien complexes **4**–**6** have very similar spectroscopic $g$ values, $g_{\perp}^{A} = [5.16–5.22]$, $g_{\perp}^{B} = [4.062–4.072]$, thus indicating that the species $A_4$, $A_5$ and $A_6$ are very similar to each other irrespective of the particular peripheral substituents of the parent porphyrin once the picdien ligand has co-ordinated. By the same token, the ESR species $B_4$, $B_5$ and $B_6$ are even more alike.

It seems then that the picdien axial ligand has the ability, by virtue of its co-ordination to these porphyrins, to produce only two ligand-field $Fe^{III}$ environments A and B, in the complexes. To study further the characterization of the two species A and B, extensive ESR calculations carried out in our laboratory show that the signals A and B for compounds **4**–**6** are not due to pure spin $S = \frac{5}{2}$ or $S = \frac{3}{2}$ species.[1,5,21,25,27,30,34] Moreover, the $g_{\perp}$ values of these signals are in accord with the expected $6 \leqslant g_{\perp} \leqslant 4$ values for $Fe^{III}$ species in qms.[5,25] Following the line of analysis of Maltempo *et al.*[4,26] and Reed and co-workers[1,27] and the correlation curves of % admixture *vs.* unperturbed crystal splitting ($\Delta/\lambda$) and of $g_{\perp}$ *vs.* ($\Delta/\lambda$) of these authors, we find for the complexes **4**–**6**, $(\Delta/\lambda)_A = -0.40$, $-0.69$ and $-0.33$ respectively and $(\Delta/\lambda)_B > 3.27$. The corresponding admixture (% a) percentages are $(\%\ a)_A = 56$, 64 and 53 respectively and $(\%\ a)_B < 8$ for the three complexes.

Clearly, the admixture percentage ($\%\ a_s$) of signals A is more extensive than that of signals B, which show a very small but

**Table 3** The ESR spectra of iron–porphyrins and pinch-porphyrins

| | Species A | | Species B | | Species C | | Species D |
|---|---|---|---|---|---|---|---|
| Compound | $g_{\|}$ | $g_{\perp}$ | $g_{\|}$ | $g_{\perp}$ | $g_{\|}$ | $g_{\perp}$ | $g_{iso}$ |
| **1** | 1.924 | 5.403 | 1.924 | 4.000 | 7.955 | 4.000 ± 0.008 | 2.000 |
| **4** | 1.990 | 5.172 | 1.951 | 4.072 | | | |
| **2** | | 4.890 | | 3.992 | | | |
| **5** | 1.987 | 5.222 | 1.953 | 4.067 | | | |
| **3** | | 5.137 | | 4.117 | 2.316 | | |
| **6** | 1.957 | 5.238 | 1.957 | 4.100 | | 2.000 | |

measurable admixture of the $|\frac{5}{2}\rangle$ state into the $|\frac{3}{2}\rangle$ state. Taking into account that reported porphyrin–$Fe^{III}$ compounds[32–35] clearly show a correlation between the spin state and the out-of-plane position of the iron ion, that is to say, compounds with $Fe^{III}$ in high-spin $S=\frac{5}{2}$ state have the metal ion out-of-plane by as much as 0.3–0.5 Å[26,27] and compounds with low-spin $S=\frac{1}{2}$ state have the metal ion almost in the plane, all other spin states are in an intermediate out-of-plane position. Hence, the two paramagnetic species A and B stabilized by the picdien ligand axially co-ordinated to the three different porphyrins **4**–**6**, should correspond to the intermediate out-of-plane position (A) and the very small out-of-plane position (B), respectively.

The three novel complexes **4**–**6** made from porphyrin–$Fe^{III}$ co-ordinated axially to the ligand picdien, define a new family of iron–porphyrin compounds, pinch-porphyrins. The presence of the axially co-ordinated picdien ligand diminishes the distortion of the ligand field present in the parent compounds.

The $^1$H NMR frequency shifts and the Curie law plots of complexes **4**–**6** indicate that the picdien pyridyl groups have induced some intermediate spin $S=\frac{3}{2}$ character into these compounds. They are spin admixed $S=\frac{5}{2}$, $S=\frac{3}{2}$ six-co-ordinated systems.

The ESR spectra of the three parent porphyrins **1**–**3** were quite different from each other, indicating the effect that the peripheral proto, meso and deutero substituents have on the magnetic state of the iron(III) ion of each compound. These compounds stabilize a variety of magnetic species and present to the picdien chain ligand two inequivalent co-ordination sites. In all three cases, they give rise to simpler ESR spectra. The spin admixture percentages for species A and B were calculated and the admixture percentage of signals A is higher than that of signals B.

The picdien co-ordination strength follows the opposite order to the ratio of the areas of the ESR signals B : A. These trends are similar to the peroxidase activity order shown by these complexes. The more active catalytic species is the one that corresponds to the lowest strength co-ordination and the largest ESR B signal. This in turn corresponds to the very close position of the $Fe^{III}$ to the plane presenting very small but measurable qms $|\frac{5}{2}\rangle$, $|\frac{3}{2}\rangle$ states.

### Study of the catalytic effects on peroxidase activity of the compounds 1–6

**Kinetics.** Numerous model compounds of peroxidases have been synthesized starting from porphyrin–$Fe^{III}$ in order to study their structural, electronic and magnetic characteristics and their peroxidase activity.[8–24]

In order to value the effect that the picdien axial ligand has in the pinch-porphyrins **4**–**6** on their peroxidase-like activity, we studied the catalytic behavior of the compounds **1**–**6**. The experimental conditions were such that the steady-state oxidation of guaiacol (hydrogen donor) is zero order with respect to guaiacol (2-methoxyphenol) concentration. The oxidant was hydrogen peroxide.

Steady-state kinetics for the normal horseradish peroxidase (HRP) cycle, may be represented by equations (1)–(3) where

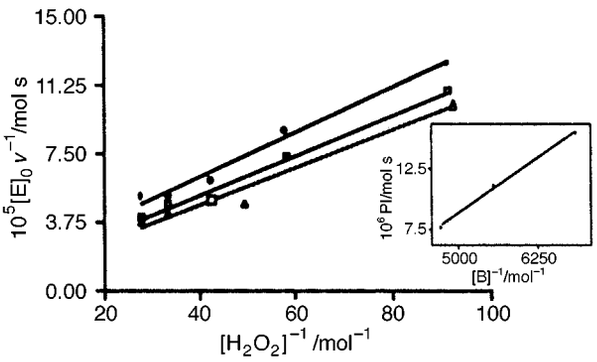


**Fig. 10** Plots of ($[E]_0\,v^{-1}$) *vs.* 1/[A]. For compound **6**: $[E]_0 = 0.017$ mmol, [guaiacol] = 0.1550, 0.1930 and 0.2307, $[H_2O_2] = 10.86$–42.41 mmol. Reaction volume was 3 ml; temperature 25 ± 0.01 °C, pH = 6.5. Inset shows a secondary plot with abscissa interception ($1/K_B$) at $2.8 \times 10^3$ mol$^{-1}$, ordinate interception ($1/k_{cat}$) at $1.1 \times 10^{-5}$ mol s and a slope ($K_B/k_{cat}$) of $3.9 \times 10^{-9}$ mol$^2$ s

$$HRP + H_2O_2 \xrightarrow{k_1} HRP\text{-}I + H_2O \quad (1)$$

$$HRP\text{-}I + AH_2 \xrightarrow{k_2} HRP\text{-}II + {}^{\bullet}AH \quad (2)$$

$$HRP\text{-}II + AH_2 \xrightarrow{k_3} HRP + {}^{\bullet}AH \quad (3)$$

HRP-I and HRP-II are compounds I and II, $AH_2$ is a reducing substrate, and $^{\bullet}AH$ a free radical product.[49]

The pattern of two reactants and two products, *i.e.* a ping-pong mechanism,[49] was utilized since the pinch-porphyrin kinetics indicate substrate inhibition by peroxide.[50] The conventional ping-pong scheme is shown in equations (4) and (5)[49]

$$E + A \rightleftharpoons EA \longrightarrow F + P \quad (4)$$

$$F + B \rightleftharpoons FB \longrightarrow E + Q \quad (5)$$

where E (resting enzyme) = iron(III)–porphyrin–picdien complexes, A and B (reactants) = $H_2O_2$ and guaiacol, F (covalently modified enzyme) = compound I, and P and Q (products) = $H_2O$ and oxidation products.

The initial rate data were analyzed using equation (6). In this

$$[E]_0\,v^{-1} = K_A/k_{cat}(1/[A] + 1/k_{cat}\{1 + (K_B/[B])\}) \quad (6)$$

case, $[E]_0$ (total enzyme concentration) = total iron(III)–porphyrin–picdien complex, $v$ = initial rate, $K_A$ and $K_B$ = Michaelis constants with respect to $H_2O_2$ and guaiacol, $k_{cat}$ = theoretical maximum rate constant. The $[E]_0\,v^{-1}$ *vs.* 1/[A] plot is a straight line for one constant and specific concentration of guaiacol [B]. For each new concentration of [B] a parallel straight line is obtained (Fig. 10). All such plots are called primary plots. The ordinate intercepts of these parallel straight lines are given by equation (7). The plot obtained using this

$$\text{Primary intercept (PI)} = (K_B/k_{cat})[B]^{-1} + 1/k_{cat} \quad (7)$$

**Table 4** Michaelis and theoretical maximum rate constants experimentally obtained

| Complex | $K_A$/mol | $K_B$/mol | $k_{cat}$/mol$^{-1}$ s$^{-1}$ |
|---|---|---|---|
| **1** | $2.0 \times 10^{-2}$ | $2.5 \times 10^{-4}$ | $1.3 \times 10^{4}$ |
| **4** | $9.1 \times 10^{-2}$ | $2.3 \times 10^{-3}$ | $7.6 \times 10^{6}$ |
| **2** | $1.2 \times 10^{-2}$ | $9.1 \times 10^{-5}$ | $1.7 \times 10^{3}$ |
| **5** | $8.6 \times 10^{-2}$ | $7.6 \times 10^{-4}$ | $4.4 \times 10^{5}$ |
| **3** | $2.9 \times 10^{-1}$ | $1.6 \times 10^{-4}$ | $3.9 \times 10^{3}$ |
| **6** | $1.0 \times 10^{-1}$ | $3.5 \times 10^{-4}$ | $9.0 \times 10^{4}$ |

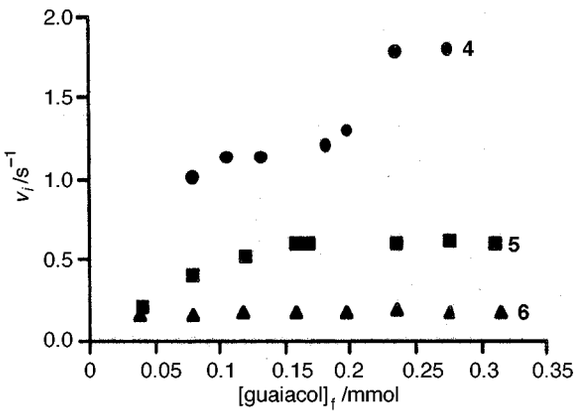


**Fig. 11** Plots of $v_i$ *vs.* [guaiacol]$_f$ for compounds **4**–**6**. Initial rate values were in a steady state in the guaiacol concentration range 0.11 to 0.20 mmol for all three complexes

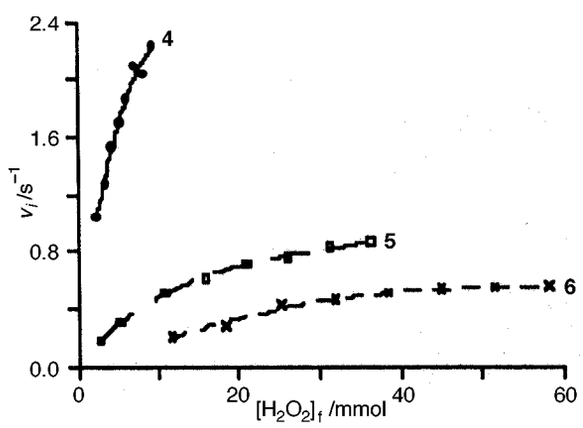


**Fig. 12** Plots of $v_i$ *vs.* [$H_2O_2$]$_f$ for complexes **4**–**6**. The initial rate values increased with the peroxide concentration. The concentration of the complex is close to saturation. Typical Michaelis–Menten behavior is observed for all three complexes

equation is called a secondary plot. From the secondary plot of primary intercept values, obtained from equation (6) *vs.* [B]$^{-1}$, both $K_B$ (1/abscissa interception) and $k_{cat}$ (1/ordinate interception) may be calculated [equation (7)]. Hence, using the value of $k_{cat}$, $K_A$ can be obtained from parallel slopes ($K_A/k_{cat}$) using equation (6). Both the primary and secondary plots have finite intercepts.[49]

In general for all porphyrins, the initial velocity values were steady state in the final guaiacol concentration range, [guaiacol]$_f$, 0.11–0.20 mmol for complex **4** and 0.10–0.40 mmol for the other complexes (Fig. 11). When the final peroxide concentration, [$H_2O_2$]$_f$, was increased from 2.3 to 20 mmol the initial rate values also increased for compounds **4** and **5**. The same effect was observed for **6** at final oxidant concentration 11.5–37 mmol (Fig. 12). In both cases, saturation was observed at higher concentrations.

When the concentration of iron–porphyrin–picdien and iron–porphyrin complexes was increased, the initial rate values also rose and saturation was never observed (Fig. 13). Kinetic studies under the same conditions were made with picdien-free

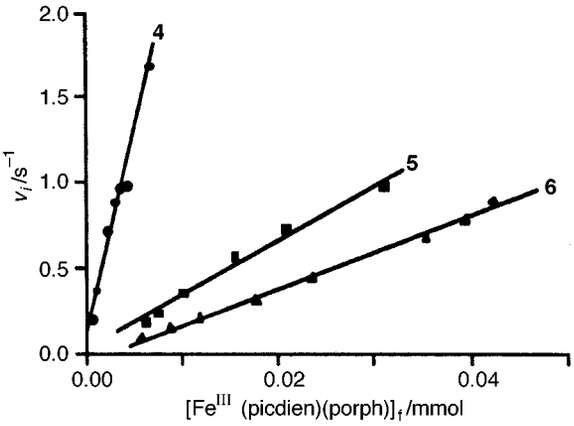


**Fig. 13** Plots of $v_i$ *vs.* [Fe$^{III}$(picdien)(porph)]$_f$ for complexes **4**–**6**. The initial rate values increase as the concentration of complex **4**–**6** was increased. Saturation was not observed

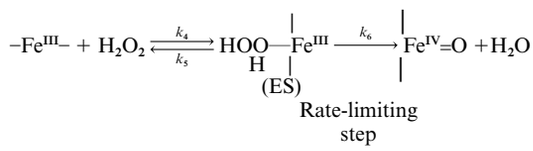


**Scheme 1**

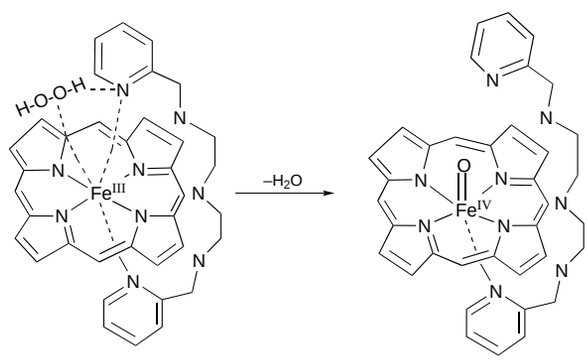


**Scheme 2**

iron–porphyrins in order to determine the effect of the presence of the axial ligand in the catalytic capacity of the model complexes. The results are in Table 4.

The values of Michaelis constants relative to peroxide for porphyrin–iron alone (complexes **1** and **2**) are shorter than for porphyrin–iron–picdien **4** and **5**. The opposite is true for **3** and **6**.

The information given by the Michaelis constants on the three picdien complexes is very similar to that of the parent iron–porphyrins. The $K_A$ values for complexes **4** and **5** indicate a low affinity of each for hydrogen peroxide and an even lower one for **6**. Hence, a high concentration of $H_2O_2$ was needed in the experiments. This indicates that the dissociation constant of the ES complex (Scheme 1) is equal to $K_A$ if $k_6$ is much smaller than $k_5$, $K_A$ is a measure of the strength of the ES complex: a high $K_A$ indicates weak binding; a low $K_A$ indicates the opposite. In this case $k_6 \ll k_5$ and $K_A = k_5/k_4$.[11] The co-ordination of the oxidant to the metal is difficult in these complexes, it is probably caused by the pyridyl group occupying the axial site, which mimics the distal histidine. As a consequence, it is proposed that temporary loss of co-ordination of one of the pyridyl groups is necessary in order to get the intermediate compound I.[51]

The guaiacol Michaelis constants, $K_B$, are smaller than the others mentioned above ($K_A$). This is consistent with the proposed mechanism of native peroxidases in which once the enzyme is oxidized, it oxidizes the substrate.[51] The proposed movement of the pinch is represented in Scheme 2.

The values of the theoretical maximum rate constant, $k_{cat}$, and the cyclic behavior of the pinch-porphyrins show that the guaiacol oxidation is a faster reaction than the iron–porphyrin autooxidation[52] in the order **4 > 5 > 6**. This means that the oxidized complex $[Fe^{IV}=O(picdien)(porph)]^{\cdot +}$ is more stable for complex **4** than for **5** and **6**.

We have developed a new kinetic model system of peroxidases, namely pinch-porphyrins, whose axial ligand picdien increased 100 times the catalytic activity of the parent iron–porphyrin compounds. The high-oxidation state compound which oxidizes the guaiacol [π-cationic iron(IV) radical] is quite stable and its stability is ascribed to the fact that the picdien ligand remains bonded to the iron by one pyridyl group, avoiding irreversible metal oxidation and thus favoring catalytic activity for many cycles.

Proton NMR, optical and ESR spectroscopies are used in combination here to show that the iron environment of the porphyrin complexes **4**–**6** are significantly altered by picdien binding and that the spin state of the iron(III) is a mixed quantum intermediate state that correlates with $r_{Fe}$ and the catalytic activity.

These magnetic and electronic properties and the catalytic activity shown by compounds **4**–**6**, especially **4**, have a strong resemblance to those of the native HRP enzymes. The magnetic changes found strongly support the idea of a sensitive fine tuning mechanism during the biochemical activity of the native enzymes where the intermediate spin state plays a central role.

## Experimental

### Instruments

Titration and other spectrophotometric measurements were performed on a UV/VIS/NIR Shimadzu 3100 spectrophotometer at 25 °C; NMR measurements were carried out on a Bruker DMX500 instrument using a five millimeters inverse detection probe at variable temperature and at 300 MHz; ESR spectra were recorded on a JEOL JES-RE3X spectrometer at liquid-nitrogen temperature. The microwave X-band (≈9.8 GHz) was used.

### Materials

Spectrophotometric and kinetic measurements were made in anhydrous methanol. The iron–porphyrins were prepared as described in previous studies.[53,54] The compound 1,9-bis-(2-pyridyl)-2,5,8-triazanonane (picdien) was prepared by the method of Ahmed *et al.*[55] The kinetic studies were made in aqueous 20.1 mmol solution of guaiacol; the porphyrin–iron methanolic solutions were 0.015–0.030 mmol and the hydrogen peroxide solution was 1.4–1.6 mol.

### Preparation of iron–porphyrin–picdien complexes

All complexes were synthesized using the same method. At 25 °C the porphyrin was dissolved in methanol and treated with picdien in equimolecular quantities. The mixture was stirred for 6 h. The spectroscopic and kinetic studies were performed directly on the reaction solutions.

### Kinetic studies

Rate determination of iron–porphyrin-catalyzed oxidation of guaiacol with hydrogen peroxide was carried out as previously described for horseradish peroxidase,[56] the oxidation product concentration was determined by optical spectrophotometry. In order to observe the oxidation products, the reaction (guaiacol with peroxide in the presence of each pinch-porphyrin complex) was observed through UV/VIS spectroscopy with time intervals of 90 s. It is important to note that the complexes were stable throughout the studies. The pH range was 6.5–7.0. The final concentrations being 0.017, 0.160 and 11.27 mmol respectively.

## References


1 C. A. Reed and F. Guiset, *J. Am. Chem. Soc.*, 1996, **118**, 3281.
2 M. M. Maltempo, T. H. Moss and M. A. Cusanovich, *Biochim. Biophys. Acta*, 1974, **342**, 290.
3 S. Ozaki, T. Matsui and Y. Watanabe, *J. Am. Chem. Soc.*, 1996, **118**, 9784.
4 M. M. Maltempo and T. H. Moss, *Q. Rev. Biophys.*, 1976, **9**, 181.
5 C. E. Schulz, R. Rutter, J. T. Sage, P. G. Debrunner and L. P. Hager, *Biochemistry*, 1984, **23**, 4743.
6 B. G. J. M. Bolscher, H. Plat and R. Wever, *Biochim. Biophys. Acta*, 1984, **784**, 177.
7 L. Casella, M. Gullotti, S. Poli, R. P. Ferrari, E. Laurenti and A. Marchesini, *BioMetals*, 1993, **6**, 213.
8 G. La Mar, *Biological Applications of Magnetic Resonance*, Academic Press, New York, 1979, 305.
9 H. A. O. Hill and K. G. Morallee, *J. Am. Chem. Soc.*, 1972, **94**, 731.
10 M. Zobrist and G. N. La Mar, *J. Am. Chem. Soc.*, 1978, **100**, 1944.
11 T. G. Traylor, W. A. Lee and D. V. Stynes, *J. Am. Chem. Soc.*, 1984, **106**, 755.
12 H. M. Goff and M. A. Phillippi, *J. Am. Chem. Soc.*, 1983, **105**, 7567.
13 G. N. La Mar, D. B. Viscio, K. M. Smith, W. S. Caughey and M. L. Smith, *J. Am. Chem. Soc.*, 1978, **100**, 8085.
14 D. L. Budd, G. N. La Mar, K. C. Langry, K. M. Smith and R. Nayyir-Mazhir, *J. Am. Chem. Soc.*, 1979, **101**, 6091.
15 R. J. Kurland, R. G. Little, D. G. Davis and Ch. Ho, *Biochemistry*, 1971, **12**, 2237.
16 T. G. Traylor and R. Popovitz-Biro, *J. Am. Chem. Soc.*, 1988, **110**, 239.
17 J. T. Groves, R. C. Haushalter, M. Nakamura, T. E. Nemo and B. J. Evans, *J. Am. Chem. Soc.*, 1981, **103**, 2884.
18 H. Fuji, *J. Am. Chem. Soc.*, 1993, **115**, 4641.
19 T. Castner, jun., G. S. Newell, W. C. Holton and C. P. Slichter, *J. Chem. Phys.*, 1960, **32**, 668.
20 R. D. Dowsing and J. F. Gibson, *J. Chem. Phys.*, 1969, **50**, 294.
21 C. Schaefer, M. Momenteau, J. Mispelter, B. Loock, C. Huel and J.-M. Lhoste, *Inorg. Chem.*, 1986, **25**, 4577.
22 F. S. Woo and H. C. Kelly, *Inorg. Chim. Acta*, 1994, **225**, 255.
23 P. Jones, D. Mantle and I. Wilson, *J. Chem. Soc., Dalton Trans.*, 1983, **29**, 1434.
24 R. E. Rodriguez, F. S. Woo, D. A. Huckaby and H. C. Kelly, *Inorg. Chem.*, 1990, **29**, 1438.
25 H. M. Goff, E. T. Shimomura and M. A. Phillippi, *Inorg. Chem.*, 1983, **22**, 66.
26 M. M. Maltempo, *J. Chem. Phys.*, 1974, **61**, 2540.
27 C. A. Reed, T. Mashiko, S. P. Bentley, M. E. Kastner, W. R. Scheidt, K. Spartalian and G. Lang, *J. Am. Chem. Soc.*, 1979, **101**, 2948.
28 A. Boersma and H. M. Goff, *Inorg. Chem.*, 1982, **21**, 581.
29 B. J. Kennedy, K. S. Murray, P. R. Zwack, H. Homborg and W. Kalz, *Inorg. Chem.*, 1986, **25**, 2539.
30 L. N. Ohlhausen, D. Cockrum, J. Register, K. Roberts, G. J. Long, G. L. Powell and B.B. Huitchinson, *Inorg. Chem.*, 1990, **29**, 4886.
31 M. Kastner, T. Mashiko and C. A. Reed, *J. Am. Chem. Soc.*, 1978, **100**, 666.
32 H. Ogoshi, H. Sugimoto and Z. Yoshida, *Biochim. Biophys. Acta*, 1980, **621**, 19.
33 D. A. Summerville, I. A. Cohen, K. Hatano and W. R. Scheidt, *Inorg. Chem.*, 1978, **17**, 2906.
34 D. H. Dolphin, J. R. Sams and T. B. Tsin, *Inorg. Chem.*, 1977, **16**, 711.
35 H. Masuda, T. Taga, K. Osaki, H. Sugimoto, Z. Yoshida and H. Ogoshi, *Inorg. Chem.*, 1980, **19**, 950.
36 G. P. Gupta, G. Lang, Y. J. Lee, R. Scheidt, K. Shelly and C. A. Reed, *Inorg. Chem.*, 1987, **26**, 3022.
37 M. Zerner, M. Gouterman and H. Kobayashi, *Theor. Chim. Acta*, 1966, **6**, 363.
38 J. W. Owens and Ch. O'Connor, *Coord. Chem. Rev.*, 1988, **84**, 1.
39 M. Gouterman, in *The Porphyrins*, ed. D. Dolphin, Academic Press, New York, 1978, vol. 3. p. 69.
40 F. Adar, in *The Porphyrins*, ed. D. Dolphin, Academic Press, New York, 1978, vol. 4, p. 167.
41 D. Dolphin, *Isr. J. Chem.*, 1981, **21**, 67.
42 E. I. Solomon, M. L. Kirk, D. R. Gamelin and S. Pulver, *Methods Enzymol.*, 1995, **246**, 71.
43 L. B. Dugad and S. Mitra, *Proc. Indian Acad. Sci., Chem. Sci.*, 1984, **93**, 295.
44 J. D. Satterlee and J. E. Erman, *J. Am. Chem. Soc.*, 1981, **103**, 199.
45 G. N. La Mar and F. A. Walker, in *The Porphyrins*, ed. D. Dolphin, Academic Press, London, 1978, vol. 4, p. 61.
46 E. González-Vergara, M. Meyer and H. M. Goff, *Biochemistry*, 1985, **24**, 6561.

47 H. M. Goff, E. González-Vergara and M. R. Bird, *Biochemistry*, 1985, **24**, 1007.
48 S. Mazumdar, O. K. Medhi and S. Mitra, *Inorg. Chem.*, 1988, **27**, 2541.
49 H. B. Dunford, in *Peroxidases in Chemistry and Biology*, eds. J. Everse, K. E. Everse and M. B. Grisham, CRC Press, Boca Raton, FL, 1990, vol. 2, p. 2.
50 R. H. Ilgner and A. E. Woods, *Comp. Biochem. Physiol.*, *B: Comp. Biochem.*, 1985, **82**, 433.
51 A. L. Balch, *Inorg. Chim. Acta*, 1992, **198**–**200**, 297.
52 F. S. Woo, M. Cahiwat-Alquiza and H. C. Kelly, *Inorg. Chem.*, 1990, **29**, 4718.
53 A. D. Falk, *The Porphyrins and Metalloporphyrins*, Elsevier, New York, 1964, p. 800.
54 A. D. Adler, D. L. Ostfeld and E. H. Abbot, *Bioinorg. Chem.*, 1977, **7**, 187.
55 E. Ahmed, C. Chartterjee, C. J. Coosksey, M. L. Tobe and G. Williams, *J. Chem. Soc.*, *Dalton Trans.*, 1989, 645.
56 H. U. Bergmeyer (Editor), *Methods of Enzymatic Analysis*, Academic Press, New York, 1974, p. 494.

*Received* 26*th June* 1997; *Paper* 7/04516F